Identification of a Putative Membrane-Inserted Segment in the α-Toxin of *Staphylococcus aureus*†

Richard J. Ward,*,§ Michael Palmer,‖ Kevin Leonard,⊥ and Sucharit Bhakdi‖,‡

Institute for Medical Microbiology, University of Mainz, Hochhaus am Augustusplatz, D-55101 Mainz, Germany, European Molecular Biology Laboratory, Meyerhofstrasse 1, D-69117 Heidelberg, Germany, and Departmentà de Fisica, IBILCE/UNESP, São José Rio Preto-SP, Brazil

Received July 30, 1993; Revised Manuscript Received February 24, 1994®

ABSTRACT: To gain a fuller understanding of the regions of the *Staphylococcus aureus* α-toxin important in pore formation, we have used Förster dipole–dipole energy transfer to demonstrate that a central glycine-rich region of α-toxin (the so-called "hinge" region) inserts deeply into the bilayer on association of toxin with liposomes. Mutant α-toxins with unique cysteine (C) residues at positions 69 and 130 [Palmer, M., et al. (1993) *J. Biol. Chem. 268*, 11959) were reacted with the C-specific fluorophore acrylodan, which acted as an energy donor. The chosen acceptor was *N*-(7-nitrobenz-2-oxa-13-diazol-4-yl)-1,2-bis-(hexadecanoyl)-*sn*-glycero-3-phosphoethanolamine (NBD-PE). Measurement of the degree of donor quenching with increasing NBD-PE in the inner bilayer leaflet enables the distance of closest approach between donor and acceptor to be estimated. For toxin labeled with acrylodan at position 130 (in the hinge region), this distance is approximately 5 ± 2 Å, showing that the probe is close to the inner surface of the liposomes. A second probe labeled at position 69 (in the N-terminal domain) shows negligible energy transfer, indicating a distance of closest approach >40 Å. This implies that this N-terminal region remains "outside" the liposome. We propose a model in which the central region of the α-toxin inserts into the membrane and possibly participates in forming the wall of the pore.

Staphylococcus aureus is a common pathogen implicated in a wide variety of infections and is therefore of considerable clinical importance. A major factor in pathogenesis is the α-toxin, a 33.4-kDa exotoxin secreted as a monomer. The toxin damages cell membranes by binding either at low concentration to a specific acceptor or at higher concentration by adsorption (Cassidy & Harshman, 1976; Hildebrand et al., 1991). Lateral diffusion and collision of membrane-bound monomers result in formation of noncovalently linked 200-kDa hexamers, and it is these hexamers that form the functional pore [reviewed by Bhakdi and Tranum-Jensen (1987, 1991) and Bhakdi et al. (1993)].

To understand the mechanism of membrane damage it is important to have a detailed knowledge of polypeptide regions interacting with the membrane. Unlike classical integral membrane proteins, no region of pronounced hydrophobicity can be predicted from the sequence (Menestrina et al., 1992), and various models have been proposed to explain the mechanism of action (Tobkes et al., 1985; Füssle et al., 1981; Bhakdi & Tranum-Jensen, 1991; Walker et al., 1992, 1993).

Modification of cysteine residues with chromophores together with Förster dipole–dipole energy-transfer measurements has been used to estimate intra- and intermolecular distances in a number of studies [e.g., Lakey et al. (1993)]. Previous studies introducing unique cysteine residues into the wild-type α-toxin showed that biotin attached to Cys 130 becomes inaccessible to streptavidin on intact cells (Palmer et al., 1993a). The possibilities was therefore considered that this position was protected due to membrane insertion. In this study, we use these mutants labeled specifically at the SH groups with acrylodan, together with fluorescence spectroscopy to measure energy transfer to an acceptor on the lipid head groups located on the inner leaflet of the lipid bilayer in liposomes. From calculations to find the distance of closest approach of donor and acceptor, we have identified a central region of the protein that is initially exposed to solvent and becomes deeply inserted into the lipid bilayer on association of the toxin with artificial membranes.

MATERIALS AND METHODS

Preparation of Protein. Site-directed mutagenesis was done previously (Palmer et al., 1993a,b), yielding two single-cysteine-containing mutants, G130C and S69C. Recombinant mutant and wild-type α-toxins were prepared from culture supernatants of *S. aureus* strain Y1090 transformed with the plasmid pDU1212 carrying the wild-type or mutant toxin DNA insert. Both mutant proteins were labeled with acrylodan as described previously (Prendergast et al., 1983), giving α-toxin labeled with acrylodan [6-acryloyl-2-(dimethylamino)naphthalene; Molecular Probes Inc., Eugene, OR] at position 130 (C130ac) and at position 69 (C69ac).[1] The efficiency of acrylodan labeling was assessed with a dithionitrobenzoate assay (Ellman, 1959); the A_{412} (as with all other absorbance values reported) was measured with a double-beam spectrophotometer (Cecil 4000). In both cases labeling was found to be >95%.

Preparation of Liposomes. Class 1 EYPC and EYPG were obtained from Lipid Products (Nutfield Nurseries, Surrey, England). Cholesterol was obtained from Sigma (Sigma

† This work was supported by the Deutsche Forschungsgemeinschaft, Grant SFB 311.

§ IBILCE/UNESP.
‖ University of Mainz.
⊥ European Molecular Biology Laboratory.
‡ To whom reprint requests should be sent.

® Abstract published in *Advance ACS Abstracts,* May 15, 1994.

[1] Abbreviations: EYPC, egg yolk phosphatidylcholine; EYPG, egg yolk phosphatidylglycerol; HEPES, 2-[4-(2-hydroxyethyl)-1-piperazinyl]-ethanesulfonic acid; NBD-PE, *N*-(7-nitrobenz-2-oxa-1,3-diazol-4-yl)-1,2-bis(hexadecanoyl)-*sn*-glycero-3-phosphoethanolamine; C69ac, acrylodan-labeled S69C α-toxin; C130ac, acrylodan-labeled G130C α-toxin; SDS–PAGE, sodium dodecyl sulfate polyacrylamide gel electrophoresis.

0006-2960/94/0433-7477$04.50/0

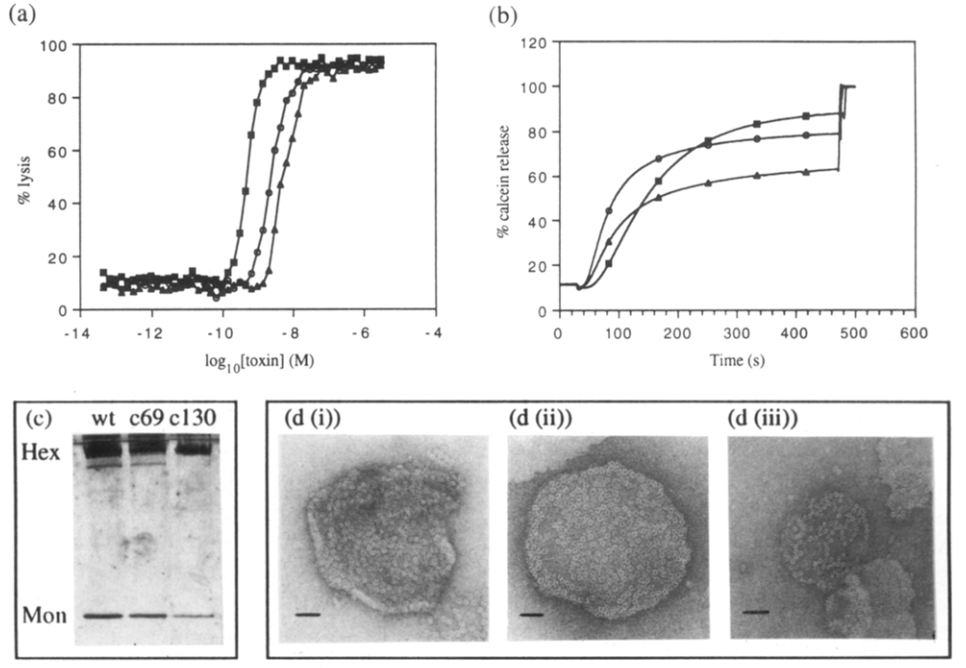

FIGURE 1: Assays of protein activity (a) Hemolytic titration on rabbit erythrocytes. Exact conditions are described in text. Curves are wild-type (●), C69ac (▲), and C69ac (■). (b) Release of entrapped calcein from liposomes of 4:1:5 EYPC:EYPG:cholesterol at a protein:lipid ratio of 1:500. Curves are labeled as in part a. (c) 10% SDS–PAGE gel of wild-type, C69ac, and C130ac samples incubated with lipid at a protein:lipid ratio of 1:500 for 45 min at room temperature. Samples were dissolved in SDS buffer and loaded immediately without heating. Gels were silver stained; monomer and hexamer bands are indicated. (d) Electron micrographs of samples used in part c in 1% UAc_2 negative stain; scale bar 50 nm.

Chemie GmbH, Germany) and was twice purified by recrystallization from methanol. All lipids appeared pure as assayed by thin-layer chromatography. Lipids were measured into clean glassware at a EYPC:EYPG:cholesterol molar ratio of 4:1:5, dried to a thin film under a stream of dry N_2, and vacuum desiccated for 1 h. Liposomes were made by reverse phase evaporation (Szoka & Papahadjopoulos, 1978) in a standard buffer (in mM, NaCl 150, HEPES 20, pH 7.4), and passed through a 400-nm polycarbonate filter. After the treatment with polycarbonate filters, the liposomes were size fractionated using a Sepharose 4B-CL column (Pharmacia LKB, Uppsala, Sweden).

For energy-transfer experiments, *N*-(7-nitrobenz-2-oxa-1,3-diazol-4-yl)-1,2-bis(hexadecanoyl)-*sn*-glycero-3-phosphoethanolamine (NBD-PE) was chosen as the acceptor. NBD-PE was obtained from Molecular Probes Inc. (Eugene, OR) and used as supplied. Liposomes containing NBD-PE were prepared as described above, except in addition NBD-PE was added to the lipid mixture at 0.25–2.00% molar ratios. After the filtration step, liposomes were treated with 10 mM dithionate, resulting in liposomes with only the inner leaflet containing the NBD-PE (McIntyre & Sleight, 1991). All NBD-PE liposome preparations were routinely checked by monitoring NBD-PE emission on dithionate treatment, and only those preparations showing a stable signal at 50% of the initial value were used in this study. Gel filtration was used as before to size fractionate the liposomes and, in this case, to remove excess dithionate. For marker release experiments, liposomes were prepared with the addition of 50 mM calcein (Sigma GmbH) to the standard buffer. The gel filtration step separated liposomes-entrapped calcein from free marker. In all cases the phospholipid concentration was assayed by the method of Gerlach and Deuticke (1963) and a cholesterol esterase/cholesterol oxidase enzymatic assay kit (Boehringer Mannheim, Mannheim, Germany).

Assays of Labeled Protein Activity. Hemolytic titrations of rabbit erythrocytes with C69ac, C130ac, and wild-type toxin were performed as previously described (Füssle et al., 1981). To assess the pore-forming activity in the liposome system used in this study, calcein-loaded liposomes were incubated at 25 °C with labeled and wild-type toxin at a protein:lipid molar ratio of 1:500. During the incubation the fluorescence emission of calcein was monitored using an SLM 8000 (SLM Instruments Inc., Urbana, IL) at 520 nm; the excitation wavelength (λ_{ex}) was 480 nm. As depicted in Results (Figure 1b), marker release from the toxin-treated liposomes approached 90%, indicating that the majority of vesicles were unilamellar. Additional liposomes were made in standard buffer alone and incubated with labeled and wild-type toxins. Samples of each were prepared for electron microscopy by negative staining with 1% uranyl acetate on carbon-coated electron microscope grids. Samples were examined in a Phillips EM400T operating at 80 kV and 36000× magnification. Aliquots of the same preparation were mixed with an SDS loading buffer without boiling and run on 7.5% SDS–PAGE (Laemmli, 1970), and gels were silver stained. Binding of protein to liposomes was assayed by flotation of liposomes in sucrose gradients and assaying all fractions for protein content with SDS–PAGE (Füssle et al., 1981).

Spectroscopy. Spectra were recorded using an SLM 8000 with a xenon lamp source. Except where indicated, the temperature was regulated at 25 °C by a thermostated water recirculator. Typically, 150–200 pmol of C130ac or C69ac was added to 400 μL of buffer in a silanized cuvette, giving a final protein concentration of 0.4–0.5 μM. For experiments involving incubation with lipids, a constant volume of liposome suspension needed for a protein:lipid ratio of 1:500 was added, so keeping the dilution correction constant between experiments. The protein/lipid mixture was incubated for 45 min at room temperature. Excitation and emission spectra of protein both with and without lipid were measured with λ_{ex} of 365 nm. Excitation and emission bandwidths were 4 and 8 nm, respectively, and all spectra were corrected with a buffer blank. In the fluorescence quenching experiments, liposomes

containing increasing molar ratios of NBD-PE (see previous section) were incubated with labeled toxin and the emission spectra recorded at λ_{ex} of 365 nm as outlined above. Details of spectra analysis are given in Results.

Polarization measurements were made using an SLM 8000 in a "T" configuration equipped with Glan-Thompson calcite prism polarizers. Vertically polarized emission was passed through a holographic diffraction grating monochromator, and horizontally polarized emission was passed through cutoff filters (Schott GmbH, Germany) at 400 and 515 nm for acrylodan and NBD-PE, respectively. Each measurement was taken as the final value of a running average of four acquisitions each with a 10-s integration time. Polarization (P) is defined as

$$P = (R_{vv} - CR_{vh})/(R_{vv} + CR_{vh}) \quad (1)$$

where R_{vv} and R_{vh} are the relative fluorescence intensities of the horizontal and vertical emission components on excitation with vertically polarized light, and C is a machine dependent correction factor measured with horizontally polarized excitation. From this value, the anisotropy (r) can be calculated according to

$$r = 2P/(3 - P) \quad (2)$$

The limiting anisotropy, r_0, is defined as the anisotropy in a solution of infinite viscosity (see Results for theory). Experimentally, r_0 of C60ac and C130ac in solution was determined by increasing buffer viscosity with appropriate volumes of buffered 75% sucrose (Merck, Darmstadt, Germany). The r_0 of NBD-PE incorporated into liposomes at a 1% molar ratio was assessed by measuring anisotropies and excited-state lifetimes by stepwise increases of sample temperature from 0 °C to 35 °C. The r_0 of C69ac and C130ac in association with liposomes and the transfer anisotropies of donors (C69ac or C130ac) to acceptor (NBD-PE) were determined in a similar manner. Anisotropy data from these experiments were used in a Perrin plot (Perrin, 1924), and a linear extrapolation was made to the anisotropy at infinite viscosity (see Results for details).

Since temperature was varied in the determination of r_0, the fluorescence decay lifetimes were measured by time-correlated single-photon counting. The output of a pulsed Nd:YAG laser was frequency doubled to 532 nm, and a tunable dye laser (LC 7100) was synchronously pumped to produce 700-nm output pulses. The output was frequency doubled, producing a final λ_{ex} at the sample of ~350 nm. Emission was recorded through a monochromator by a photomultiplier. Since the absolute chromophore concentration is low, in order to obtain reliable counting statistics data collection was made over a period of 1000 s. Lifetime decay values were calculated using a nonlinear least squares iterative convolution method as implemented on an IBM-PC. The instrument response allows resolution of lifetimes greater than 8 ps.

The quantum yield of the acrylodan complexed to protein was determined by a comparative method (Hudson & Weber, 1973), using 10 μM quinine sulfate dissolved in 0.1 N H_2SO_4 as a reference. The quantum yield of the reference at an excitation wavelength of 365 nm was taken to be 0.546 (Demas & Crosby, 1971). All spectra were corrected for inner filter effects.

RESULTS

Activity of Labeled Mutant Protein. Figure 1 shows a panel of the results of four assays used to measure activity. Figure 1a shows the hemolytic titration on rabbit erythrocytes of C69ac, C130ac, and wild-type toxin. In all cases, 100% lysis was seen by 10 nM, indicating that the modifications did not seriously affect the binding of the toxin to the high-affinity binding sites on the erythrocytes (Hildebrand et al., 1991). However, the toxin concentration needed for 50% lysis was increased in the case of C69ac, from 2 nM in the case of wild-type to 4 nM with C69ac. The opposite effect was seen with C130ac, where the concentration of the toxin needed for 50% lysis decreased to ~600 pM.

Figure 1b shows the effect of C69ac and C130ac on entrapped calcein release compared to wild-type toxin on liposomes. Modification at the C69ac position results in a slightly reduced rate and extent of calcein release compared to the wild-type. With C130ac, after a short 20–30-s time lag, a more prolonged, but slightly slower release is seen than with wild-type. The results show that although there are differences in the rates and final fraction of marker released, both modified proteins show the ability to form functional pores in liposomes. We cannot exclude that the sometimes incomplete calcein release was due to the presence of contaminating multilamellar vesicles. To avoid interference of such vesicles with fluorescence energy transfer studies, only preparations displaying a 50% decrease in NBD-PE emission on dithionate treatment were used in those experiments.

Figure 1c shows the result from SDS–PAGE of liposomes incubated with both modified toxins and wild-type. The hexamer and monomer bands are indicated and show that for all proteins efficient hexamerization occurs. In particular, the majority of the toxin is converted to the hexamer form in all cases. The SDS–PAGE of the fractions from the sucrose gradients showed >90% of protein in the upper fractions in all cases, showing that the protein had bound efficiently to the liposomes. Figure 1d shows electron micrographs of liposomes after incubation with C69ac, C130ac, and wild-type toxin. In all three cases, ring structures are seen which are typical of those observed previously (Füssle et al., 1981).

Effect of Lipid on C69ac and C130ac Fluorescence. Acrylodan is a SH-specific fluorescent label, the emission spectrum of which displays a pronounced blue shift upon transfer to a hydrophobic environment. Figure 2a shows the acrylodan emission spectra of C69ac and C130ac in the presence and absence of lipid in the form of liposomes at 25 °C. Information about the immediate environment around the probes at these two positions can be derived from the more detailed analysis of the acrylodan emission spectra given in Table 1. In the case of C69ac, the λ_{max} of 476 nm indicates that the probe is situated in a partially hydrophobic environment. On addition of liposomes there are only minor changes in spectral parameters; the constant value of the Stokes shift indicates that the environment around the probe at this position has the same polarity in solution as well as when the toxin is bound to liposomes. The values for the emission intensity and lifetime remain unchanged; however, there is a small increase in quantum yield from 0.13 to 0.17. Also, on association with liposomes, a small but highly reproducible decrease of ~5% is seen in the bandwidth accompanied by an increase of ~10% in the limiting anisotropy.

In the case of the C130ac in solution, the λ_{max} of 522 nm indicates that the acrylodan is exposed to an aqueous environment at this position. The lower anisotropy seen than with C69ac indicates that the region around residue 130 is less mobile than the region around position 69, consistent with the idea of a more solvent exposed environment.

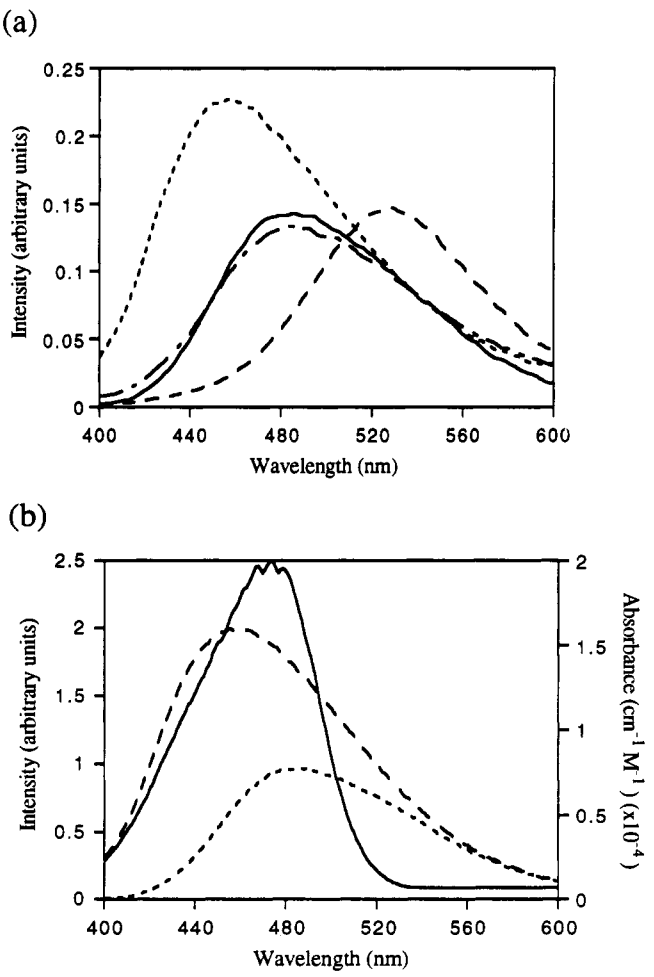

FIGURE 2: Emission spectra of acrylodan-labeled protein. (a) Fluorescence emission intensities with a λ_{ex} of 365 nm. Curves are C69ac in solution (—), C69ac incubated with liposomes (- - -), C130ac in solution (– – –), and C130ac incubated with liposomes (- - -). The protein concentration in all cases was 150–200 nM. (b) Curves used in the calculation of the overlap integral, J. The dashed lines show the emission intensities of C69ac (- - -) and C130ac (– – –) in solution, and the solid line shows the excitation spectrum of NBD-PE normalized to the absorption coefficient at 480 nm.

Table 1. Summary of the Spectral Properties of Acrylodan Coupled to C130 and C69 Mutant Toxins in Solution and Effects of the Addition of Liposomes[a]

	C69		C130	
	solution	+lipid	solution	+lipid
λ_{max} (nm)	476	476	522	450
Stokes shift (cm^{-1})	6390	6390	8120	5060
I_{lipid}/I_{soln}	1.00	0.99	1.00	1.68
quantum yield	0.13	0.17	0.15	0.40
lifetime (ns)	2.38	2.41	2.09	4.24
limiting anisotropy (r_0)	0.291	0.318	0.205	0.168

[a] The protein concentration in all cases is 150–200 pM, and when liposomes are present, the final protein:lipid ratio is 1:500. All values were determined at 25 °C.

On association with liposomes there is a large change in all spectral parameters measured, indicating considerable change in environment around the probe: the decrease in λ_{max} to 450 nm, with the large change in the Stokes shift of 3060 cm^{-1} typical of the acrylodan probe moving to a more hydrophobic environment (Prendergast et al., 1983). Consistent with this are the observed increases in decay lifetime and quantum yield. A λ_{max} of 420–430 nm was observed for acrylodan in an alkane series (dielectric constants from 1.88 to 2.07, data not shown), indicating that the environment around the C130ac is only slightly polar. The anisotropy decrease indicates that the probe has become more mobile in the hydrophobic medium than when exposed to solvent.

The results of the spectral analysis indicate that whereas the environment around the probe in C69ac remains largely unchanged when the toxin associates with lipid, the probe in the C130ac changes from a hydrophilic to a hydrophobic environment. To resolve questions as to the location of the probes in the membrane-bound form, we undertook Förster energy-transfer experiments to locate the position of the probes relative to the inner surface bilayer.

Evaluation of Föster Radius, R_0. The efficiency of Förster dipole–dipole energy transfer is given by

$$E = R_0^6/(R_0^6 + R^6) \quad (3)$$

where R is the distance separating the donor and acceptor probes and R_0 is the Förster radius.

R_0 is calculated from the expression

$$R_0\,(JQ\kappa^2 n^{-4})^{1/6}(9.79 \times 10^3) \quad (4)$$

where J is the overlap integral, Q is the quantum yield of the donor, κ^2 is the orientation factor which relates the relative motions of the donor emission and acceptor excitation vectors, and n is the refractive index of the intervening medium, for which a value of 1.4 is taken.

J is given by

$$J = \int F(\lambda)\,\epsilon(\lambda)\,\lambda^4\,d\lambda / \int F(\lambda)\,d\lambda \quad (5)$$

where, for a given value of λ, $F(\lambda)$ is the normalized donor emission and $\epsilon(\lambda)$ is the excitation spectrum of the acceptor normalized with respect to the excitation coefficient. Figure 2b shows the spectra used in the calculation of J. The normalized emission spectra of C69ac and C130ac in the presence of lipid are used as the donor spectra, along with the excitation spectrum of NBD-PE normalized to the extinction coefficient. The extinction coefficient was found experimentally by measuring the A_{470} of liposomes containing known amounts of NBD-PE and was found to be 20 100 ± 2000 M^{-1} cm^{-1}. A value of 20 100 M^{-1} cm^{-1} was used for the calculation of J.

Quantum yields were estimated as described in Materials and Methods for C69ac and C130ac in the presence and absence of lipid, and the values are shown in Table 1. In the case of C69ac there is little change when the protein binds to liposomes, whereas the C130ac there is approximately a 2.5-fold increase in the quantum yield. For distance calculations, the quantum yields of the probes in the presence of lipid were used, which are 0.17 and 0.40 for C69ac and C130ac, respectively.

An exact evaluation of κ^2 is impossible due to the dynamic nature of the probe motion. However, limiting values of κ^2 were evaluated following the theoretical and experimental procedures suggested by Dale and Eisinger (1975). Briefly, the method involves evaluation of depolarization factors which estimate the degree of rotational freedom of donor and acceptor, and a third transfer depolarization factor estimating the degree of rotation between the two. These are designated as $\langle dD \rangle$, $\langle dA \rangle$, and $\langle dT \rangle$, respectively. Depolarization factors are determined from the ratio of the limiting anisotropy and the fundamental anisotropy of the probe in question. The $\langle dD \rangle = r_{0D}/r_{fD}$ and $\langle dA \rangle = r_{0A}/f_{fA}$, where r_{0D} and r_{0A} are the limiting anisotropies of the donor and the acceptor, and

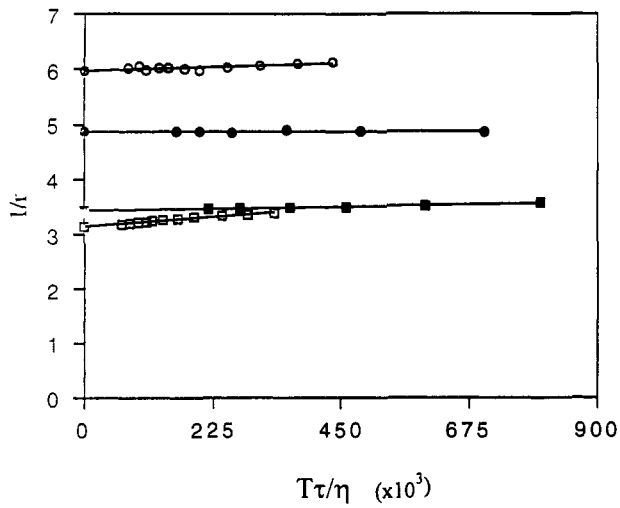

FIGURE 3: Perrin plots of $1/r$ vs $T\tau/\eta$ (where r is the measured anisotropy of the acrylodan, T is the absolute temperature value, τ is the excited lifetime decay, and η is the viscosity of the solution at temperature T). The lines represent C69ac (■) and C130ac (●) in solution and C69ac (□) and C130ac (○) incubated with liposomes. The extrapolated intercepts at the y-axis give the values for $1/r_0$ listed in Table 1.

r_{fD} and r_{fA} are the fundamental anisotropies. Figure 3 shows a series of Perrin plots for C69ac and C130ac in solution and in the presence of lipid (see Materials and Methods for experimental details). Table 1 shows the values of r_0 derived from the y-axis intercepts of these lines. The value for r_0 of 0.22 for NBD-PE incorporated into liposomes was obtained experimentally from a Perrin plot measured over the temperature range 0–35 °C (data not shown). The value of r_f for both acrylodan and NBD free in solution was assumed to be the theoretical value of 0.4 for excitation into the lowest energy band of the probes.

The transfer depolarization factor, ⟨dT⟩, is given by $r_{0A(D)}/r_{fD}$, where $r_{0A(D)}$ is the anisotropy of the acceptor emission on excitation of the donor. Anisotropies were measured by exciting C69ac and C130ac in 1% NBD liposomes at 365 nm (donor excitation) and measuring the intensity and anisotropy of NBD-PE (acceptor) emission at 540 nm. The intensity and anisotropy at 540 nm for NBD-PE liposomes alone at λ_{ex} = 365 nm was also measured, and the transfer anisotropy was found by Weber's addition law (Weber, 1966) in the form

$$r_{A(D)} = [r_{obs}(I_A + I_{A(D)}) - r_A I_A]/I_{A(D)} \quad (6)$$

where $r_{A(D)}$ and r_A are transfer and direct acceptor excitation anisotropies, r_{obs} is the observed anisotropy, and $I_{A(D)}$ and I_A are the emission intensities at λ_{ex} = 365 nm with and without labeled protein. Values for $r_{0A(D)}$ of 0.147 and 0.105 were found for C69ac and C130ac, respectively.

When the values for the three depolarization factors are known, the axial transfer depolarization factor, dT′, can be found from the expression

$$\langle dT\rangle = \langle dA\rangle dT' \langle dD\rangle \quad (7)$$

Dale and Eisinger (1975) have used a more formal treatment of eq 7 and have derived values of the orientation factor, κ^2, for a range of values of dT′, ⟨dD⟩, and ⟨dA⟩. The values are presented as a series of contour graphs, and using the experimentally determined values of ⟨dD⟩, ⟨dA⟩, and ⟨dT⟩, limiting values for κ^2 of 0.25 to 3.0 were found for C69ac in NBD-PE liposomes, and 0.35 to 2.2 for C130ac. Using

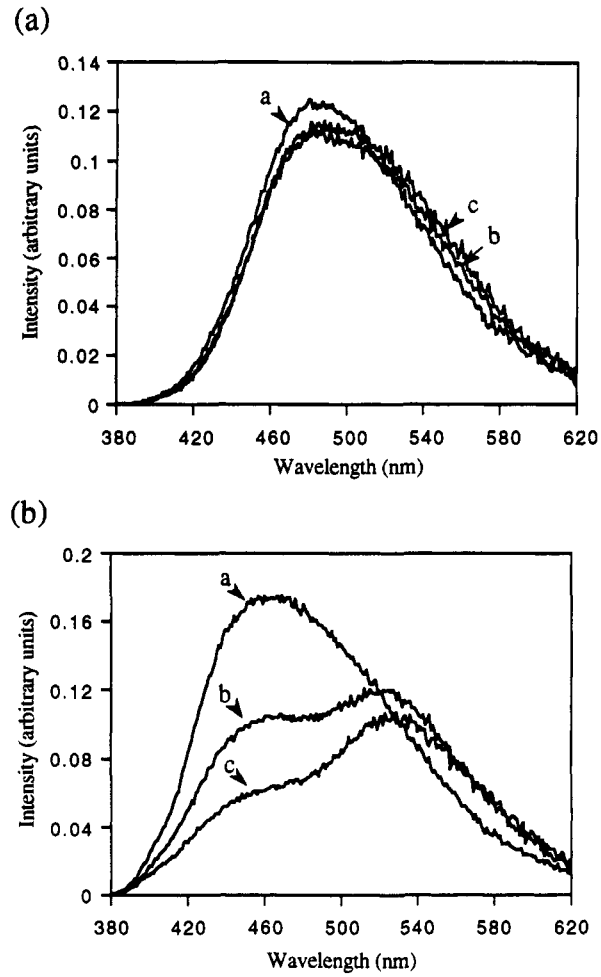

FIGURE 4: (a) Emission spectra of C69ac after incubation with liposomes containing increasing amounts of NBD-PE: λ_{ex} is 365 nm; spectrum a, 0.0% NBD-PE; spectrum b, 0.75%; spectrum c, 2% NBD-PE. (b) The same liposomes (spectra a–c) as in part 4, this time incubated with C69ac. See text for description.

these limiting values of κ^2, the maximum and minimum values of R_0 were calculated. For C69ac, R_0 = 26–39 Å, and for C130ac, R_0 = 33–43 Å. These values of R_0 were used in the estimate of the distance of nearest approach of the donor and acceptor probes, which gives a direct indication of the location of the acrylodan-labeled amino acid in the lipid bilayer.

Evaluation of the Distance of Closest Approach of Donor and Acceptor (L). Figure 4a,b shows the emission spectra of C69ac and C130ac after incubation with liposomes containing increasing amounts of NBD-PE. The λ_{max} of the NBD-PE emission alone in liposomes was found to be 540 nm, and a peak at this wavelength indicates that energy transfer is occurring. In addition, the emission of the donor will be quenched in the presence of the acceptor, and the measured intensity of the donor emission will decrease. Both these effects are seen in Figure 4b, where in the presence of NBD-PE the C130ac emission spectrum shows a clear peak at 540 nm and a decrease in the acrylodan emission. The C69ac emission spectrum shows only a "shoulder" in the same region and a much smaller decrease in donor emission. This indicates that the efficiency of energy transfer is significantly greater in the case of C130ac than C69ac. Note that although a very low level of excitation of NBD-PE is seen at λ_{ex} of 365 nm, the background of direct NBD excitation becomes appreciable at higher concentrations; therefore, all spectra were corrected using a blank containing NBD-PE liposomes alone.

Equation 3 shows that the efficiency of energy transfer is dependent on the distance separating the donor and acceptor probes. Experimentally, the efficiency of transfer is measured from either the increase in acceptor or the decrease in donor emission intensities. However, NBD-PE in liposomes has been shown to self-quench (Nichols & Pagano, 1981), so energy-transfer efficiency was measured by the decrease in donor emission intensity of C69ac or C130ac in the presence of liposomes containing increasing NBD-PE concentrations. Donor emission intensity was also measured in liposomes without NBD-PE. After suitable correction, these intensities can be used to find quantum yields of the donor in the presence of acceptor ($Q_{D(A)}$), and the transfer efficiency can be found from

$$E = 1 - (Q_{D(A)}/Q_{(D)}) \quad (8)$$

where $Q_{(D)}$ is the quantum yield of donor alone [e.g., Husten et al. (1987)].

The C130ac emission spectrum in the presence of NBD-PE (see Figure 4b) shows the emission peaks of the donor and the acceptor overlap, so to measure donor emission intensity changes, the two signals must be deconvoluted. After correction of the spectra for dilution and inner filter effects, the NBD emission due to direct excitation at 365 nm was subtracted from the spectrum as described above. The corrected quenched intensities were finally normalized with respect to protein concentration, and the transfer efficiency was calculated from eq 8.

A number of authors have developed theoretical methods for the derivation of the distance of closest approach of donor and acceptor (L) from quenched donor emission of probes in lipid bilayers (Fung & Stryer, 1978; Dewey & Hammes, 1980; Wolber & Hudson, 1979). We have used an empirical solution to the problem derived from a Monte Carlo simulation of donor and acceptor populations in a bilayer (Snyder & Freire, 1982). The analysis is further simplified since the probes are located in the inner leaflet only; therefore, no ambiguities arise from the question as to on which side of the bilayer are the acceptors that quench the donor.

The value of L will be dependent on the density of the acceptors (C), which can be expressed in terms of the number of acceptors/Å^2, calculated for all concentrations of NBD-PE using the equation

$$C = [A]/(90[PL]) \quad (9)$$

where [A] and [PL] are the concentrations of acceptor and phospholipid, respectively. The value of 90 is the area per phospholipid head group (in Å^2), in liposomes of a 1:1 EYPC: cholesterol mixture (Lecuyer & Dervichian, 1969, Lis et al., 1982).

Figure 5 shows the effect of C on the ratio $Q_{A(D)}/Q_D$ at a value of R_0 = 33 Å for both C69ac and C130ac. Also shown are the best fits to the experimental data using the method of Snyder and Freire (1982). The curve shown gives a value of L for C130ac of 8 Å and for C69ac of 65 Å. Calculation of L from the maximum and minimum values of R_0 for C130ac gives a range of values of 5–8 Å. Similar calculation for C69ac gives a value for L of 50–80 Å.

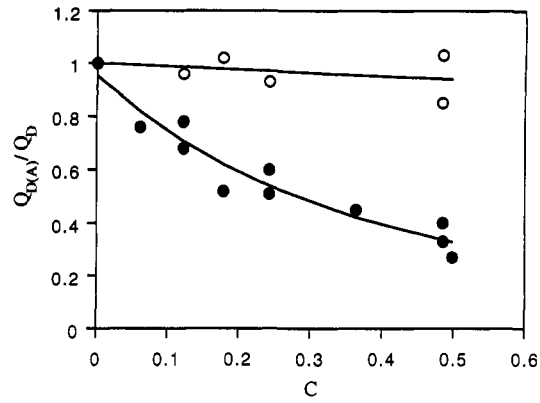

FIGURE 5: Plot of the effect of increasing acceptor density in the bilayer inner leaflet (C) on the degree of donor quenching for C69ac (○) and for C130ac (●). The solid lines are the best fits by least-squares method using the Monte Carlo simulation method of Snyder and Freire (1982) (see text for details).

DISCUSSION

We have presented evidence which supports the suggestion that the central glycine-rich region of the α-toxin is exposed to solvent in the soluble form, but becomes deeply inserted in the lipid bilayer on association with liposomes. Furthermore, the data shown here are consistent with those of previous work suggesting that the bulk of the protein remains outside of the liposomes in the function pore (Ward & Leonard, 1992).

We have assumed that the mutagenesis and chemical modification do not inactivate the toxin. As shown in Figure 1 and described in Results, the assumption is valid for the concentration of toxin used. In the case of the C69ac, the hemolytic titer is shifted slightly to higher concentrations, showing that the activity is partially reduced. The rate of release of calcein from liposomes is also reduced to ~60%, but the pore-complex rings seen with EM and the degree of hexamerization as assessed by SDS–PAGE appear normal compared to wild-type. With C130ac, the modification appears to increase toxin activity, the hemolytic titer is shifted significantly to the left, and calcein release from liposomes is higher. The monomer band on the SDS–PAGE gel is weaker and the hexamer band stronger than with wild-type, indicating an increased rate of oligomerization. The rings seen with EM appear normal. The effects gives clues as to the roles of the regions modified. Position 69 has been shown to be highly sensitive to the size of the modifying probe (Palmer et al., 1993a) and may be involved in the protomer–protomer interaction. Position 130 is more tolerant to modification, and in this case addition on a nonpolar probe increases membrane-damaging properties, indicating that changes in side-chain polarity in this region can influence toxic activity.

Considering the case of the energy-transfer experiments with C130ac, the derived value for the distance of closest approach, L, of 5–8 Å means that in absolute terms the donor must be situated somewhere on the surface of a sphere of this radius, with the acceptor at the center. It therefore follows that position 130 is situated within a maximum of 8 Å of the NBD-PE in the liposome inner leaflet. In the case of the C69ac, the value of L is 50–80 Å. Assuming a width of 40 Å for the bilayer (Lis et al., 1982; McIntosh et al., 1989), this indicates that residue 69 remains outside the outer bilayer leaflet. This conclusion is supported by the observation that biotinylated C69 on erythrocyte membranes bound externally supplied streptavidin, but that biotin-modified C130 became inaccessible to streptavidin after the toxin bound to the cells (Palmer et al., 1993a).

In order to reliably locate the position of the donor, there must be a fixed point of reference in the bilayer. The location of NBD in liposomes has been the subject of a number of previous studies (Chattopadhyay & London, 1987, 1988) and, as a result, is well defined at a distance of ~14 Å from the

bilayer center, at the polar/nonpolar transition region. We have assumed that the position of the NBD is the same in our system. To check this assumption, we measured the extinction coefficient (ϵ) of the NBD-PE both in liposomes and in an alcohol series of decreasing dielectric constant (ν). The measured value of ϵ for NBD in the liposomes used in this study was 20 100 M^{-1} cm^{-1}, and a comparison with values of ϵ for an alcohol series of decreasing dielectric constant (ν) showed that this value was reached at about $\nu = 15$ (data not shown), the value of the dielectric constant where the fatty acyl chains join the glycerol backbone (Cevc, 1990). This result is in agreement with the studies mentioned above, and such a well-defined position provides a convenient reference point for estimating distances in the bilayer using the value of L, derived from energy-transfer experiments.

We have further assumed that addition of α-toxin to liposomes does not result in redistribution of NBD probe from the inner to the outer leaflet. This is supported by the observation that whereas liposomes with NBD present in both leaflets quenched acrylodan emission in the C69ac, prolonged incubation of C69ac with dithionate-treated liposomes did not increase the NBD quenching effect.

A number of limitations must be considered in estimating the depth of a probe in the bilayer using this method, due to various factors having an influence on the value of L measured. Since the donor is labeling the protein, and the acceptor the phospholipid, steric factors affecting the interaction between the two will influence the distance of closest approach of donor and acceptor probes. One such factor will be the annulus of lipid which, as shown by NMR and EPR studies, is weakly associated with the protein (Marsh et al., 1978; Paddy et al., 1981). Those annulus-excluded acceptors will quench as predicted by assuming a random acceptor distribution, but will be restricted in their distance of closest approach to the protein. The protein-associated acceptors have a higher probability of participating in energy transfer, and so will quench with greater efficiency. The net result of these two opposing effects will depend on the affinity of the lipid and protein.

Furthermore, the proposed insertion of the loop region will bring together six acrylodan groups in the final hexamer. Snyder and Freire (1982) have analyzed the problem of nonrandom probe distribution, and they conclude that under conditions of high-efficiency quenching, such as we have demonstrated here, the effect of aggregation is greatly reduced, and we estimate the error here to be <10% in the final value of L.

In addition, the bulk of the inserted protein can also influence the value of L. For instance, the amino acid sequence around position 130 shows a cluster of charged residues (124-RTGDDT-129) immediately N-terminal of the labeled residue. Such a charge cluster is unlikely to be buried in the hydrophobic core of the membrane, and it is therefore probable that this region of the amino acid chain penetrates through the inner leaflet. Such insertion will perturb the lipid, and if the result of these rearrangements is a net movement of acceptor head groups away from the donor-labeled residues in the protein, the measured value of L will increase. An additional effect due to the bulk of inserted protein and consequent lipid displacement will be the exclusion of the acceptor probes from the area subsequently occupied by protein. This will have the effect of reducing the number of acceptors in the vicinity of the donor, and so will reduce the efficiency of the quenching, resulting in an overestimate in the value of L. Calculations by Snyder and Freire (1982) show that, for high-effiency quenching, this effect may introduce an error of <20% in the value of L.

Circular dichroism results suggest that the α-toxin has predominantly β-sheet secondary structure (Ikigae & Nakae, 1985), and previous authors have suggested that the functional pore is formed from inserted loop structures (Bhakdi & Tranum-Jensen, 1991). The mechanism of pore formation with the α-toxin requires the correct oligomerization of the protein (Walker et al., 1992). Menestrina (1992) has noted that if each subunit of the hexameric pore provides two β-strands, the resulting 12-stranded β-barrel would have the correct internal diameter to form a pore of ~11 Å, consistent with results from planar bilayer studies (Menestrina, 1986). Furthermore, inactivation of α-toxin by proteolytic nicking in the central "hinge" region has led to speculation that this central region is involved in channel formation and may insert into the membrane (Tobkes et al., 1993; Walker et al., 1993).

Here, we present more direct evidence, and we propose that, in the hexameric pore, the region of the α-toxin around residue 130 spans the bilayer. It is not known how the regions flanking residue 130 interact to form the putative membrane-spanning domain. Extended conformations such as have been proposed for transmembrane regions in a potassium channel (Yellen et al., 1991), and the acetylcholine receptor channel (Akabas et al., 1992) are conceivable. The concept that the central portion of α-toxin inserts into the bilayer is supported by results of functional complementation studies (Walker et al., 1993), where loss of activity was seen when parts of the central region were deleted. Furthermore, toxin nicked enzymatically in this region shows altered functional properties (Palmer et al., 1993b) with respect to hemolysis and pore formation in nucleated cells.

In sum, it is possible that the domain around residue 130 in fact is part of the pore wall, with major parts of the N- and C-terminal domains, comprising the bulk of the protein, remaining outside of the membrane bilayer.

ACKNOWLEDGMENT

We thank Dr. Christoph Bubeck at the Max-Planck-Institut für Polymerforschung, Mainz, and in particular Arno Domack for his expertise in helping with the lifetime decay measurements. We also thank Drs. Franc Pattus and Françoise-Gisou van der Goot for their encouragement during the work and for reading the manuscript.

REFERENCES

Akabas, M. H., Staufer, D. A., Xu, M., & Karlin, A. (1992) *Science 251*, 250.
Bhakdi, S., & Tranum-Jensen, J. (1987) *Rev. Physiol. Biochem. Pharmacol. 107*, 147.
Bhakdi, S., & Tranum-Jensen, J. (1991) *Microbiol. Rev. 55*, 733.
Bhakdi, S., Weller, U., Walev, I., Martin, E., Jonas, D., & Palmer, M. (1993) *Med. Microbiol. Immunol. 182*, 167.
Cassidy, P., & Harshman, S. (1976) *Biochemistry 15*, 2348.
Cevc, G. (1990) *Biochim. Biophys. Acta 1031*, 311.
Chattopadhyay, A., & London, E. (1987) *Biochemistry 26*, 39.
Chattopadhyay, A., & London, E. (1988) *Biochim. Biophys. Acta 938*, 24.
Dale, R., & Eisinger, J. (1975) in *Biochemical Fluorescence: Concepts* (Chen, R. F., & Edelhoch, H., Eds.) Vol. 1, pp 115–284, Marcel Dekker Inc., New York.
Demas, J. N., & Crosby, C. R. (1971) *J. Phys. Chem. 75*, 991.
Dewey, T. G., & Hammes, G. G. (1980) *Biophys. J. 32*, 1023.
Ellman, E. L. (1959) *Arch. Biochem. Biophys. 82*, 70.
Fung, B. K., & Stryer, L. (1978) *Biochemistry 17*, 5241.

Füssle, R., Bhakdi, S., Sziegoleit, A., Tranum-Jensen, J., Kranz, Y., & Wellensiek, H.-J. (1981) *J. Cell. Biol. 91*, 83.
Gerlach, E., & Deuticke, B. (1963) *Biochem. Z. 337*, 477.
Gray, G. S., & Kehoe, M. (1984) *Infect. Immun. 46*, 615.
Grossman, S. H. (1983) *Biochemistry 22*, 5375.
Hildebrand, A., Roth, M., & Bhakdi, S. (1991) *J. Biol. Chem. 262*, 12953.
Hudson, E. N., & Weber, G. (1973) *Biochemistry 12*, 4154.
Husten, E. J., Esmon, C. T., & Johnson, A. E. (1987) *J. Biol. Chem. 262*, 12953.
Ikigae, H., & Nakae, Y. (1985) *Biochem. Biophys. Res. Commun. 130*, 175.
Laemmli, U. K. (1970) *Nature 227*, 680.
Lakey, J. H., Duche, D., Gonzales-Manas, J.-M., Baty, D., & Pattus, F. (1993) *J. Mol. Biol. 230*, 1055.
Lecuyer, H., & Dervichian, D. G. (1969) *J. Mol. Biol. 45*, 39.
Lis, L. J., McAlister, M., Fuller, N., Rand, R. P., & Parsegian, V. A. (1982) *Biophys. J. 37*, 657.
Marsh, D., Watts, A., Maschke, W., & Knowles, P. F. (1978) *Biochim. Biophys. Acta 736*, 137.
Menestrina, G. (1986) *J. Membr. Biol. 90*, 177.
Menestrina, G., Belmonte, G., Parisi, V., & Morante, S. (1992) *FEMS Microbiol. Immunol. 105*, 19.
McIntosh, T. J., Magid, A. D., & Simon, S. A. (1989) *Biochemistry 28*, 17.
McIntyre, J. C., & Sleight, R. G. (1991) *Biochemistry 30*, 11819.
Nichols, J. W., & Pagano, R. E. (1981) *Biochemistry 20*, 2783.
Olafsson, A., Kaveus, U., Thelestam, M., & Hebert, H. (1992) *J. Struct. Biol. 108*, 238.
Paddy, M. R., Dahlquist, F. W., Davis, J. H., & Bloom, M. (1981) *Biochemistry 20*, 3152.
Palmer, M., Jursch, R., Weller, U., Valeva, A., Hilgert, K., Kehoe, M., & Bhakdi, S. (1993a) *J. Biol. Chem. 268*, 11959.
Palmer, M., Weller, U., Messner, M., & Bhakdi, S. (1993b) *J. Biol. Chem. 268*, 11963.
Perrin, F. (1924) *C. R. Hebd. Seances Acad. Sci. 178*, 1978.
Prendergast, F. G., Meyer, M., Carlson, G. E., Iida, S., & Potter, J. D. (1983) *J. Biol. Chem. 258*, 7541.
Shahrokh, Z., Verkman, A. S., & Shohet, S. B. (1991) *J. Biol. Chem. 266*, 12082.
Snyder, B., & Freire, E. (1982) *Biophys. J. 40*, 137.
Szoka, F., & Papahadjopoulos, D. (1978) *Proc. Natl. Acad. Sci. U.S.A.* 4184.
Tobkes, N., Wallace, B., & Bayley, H. (1985) *Biochemistry 24*, 5285.
Walker, B., Krishnasastry, M., Zorn, L., & Bayley, H. (1992) *J. Biol. Chem. 267*, 21782.
Walker, B., Krishnasastry, M., & Bayley, H. (1993) *J. Biol. Chem. 268*, 5285.
Ward, R. J., & Leonard, K. (1992) *J. Struct. Biol. 109*, 129–141.
Weber, G. (1966) in *Fluorescence and phosphorescence Analysis* (Hermles, D. M., ed.) p 217, Wiley-Interscience, New York.
Wolber, P. K., & Hudson, B. S. (1979) *Biophys. J. 28*, 197.
Yellen, G., Jurman, M. E., Abramson, T., & MacKinnon, R. (1991) *Science 251*, 250.